Submitted to the
XXXIII International Conference on High Energy Physics
July 26 - August 2, 2006, Moscow, Russia

Sessions: QCD hard interactions & Electroweak

Measurement of high-Q^2 neutral current deep inelastic scattering cross sections with a longitudinally polarised electron beam at HERA

ZEUS Collaboration

Abstract

Measurements of the neutral current cross sections for deep inelastic scattering in e^-p collisions with longitudinally polarised electron beams are presented. Single differential cross sections in Q^2, x and y, and double differential cross sections in Q^2 and x are shown in the kinematic region of $Q^2 > 200\,\mathrm{GeV}^2$ separately for positively and negatively polarised electrons. The measurements are based on an integrated luminosity of $122\,\mathrm{pb}^{-1}$ taken by the ZEUS detector in 2004 and 2005 with a centre-of-mass energy of $318\,\mathrm{GeV}$. The structure function xF_3 is also measured by combining the e^-p data with previously measured unpolarised e^+p neutral current data. The Standard Model agrees well with all measurements, with the $d\sigma/dQ^2$ measurement showing clear evidence of parity violation.

1 Introduction

Deep inelastic scattering (DIS) of leptons off nucleons is a key tool for the understanding of the structure of the proton and the form of the Standard Model (SM). The HERA *ep* collider allows the exploration of DIS at high values of the negative four-momentum-transfer squared, Q^2.

Using data taken in the years 1994-2000 the H1 and ZEUS collaborations have reported measurements of the cross sections for neutral current (NC) DIS [1–12]. These measurements extended the kinematic region covered by fixed-target experiments [13–15] to higher Q^2 and allowed the HERA experiments to probe the electroweak sector of the SM.

Since 2002, the upgraded HERA collider has delivered longitudinally polarised lepton beams to the experiments. The SM predicts that the cross section for *ep* NC DIS should exhibit a dependence on the polarisation of the incoming lepton. This effect should be most significant at high Q^2 where the Z^0 boson exchange becomes important.

Measurements of e^+p NC DIS cross sections with longitudinally polarised positron beams have been published by the ZEUS collaboration [16]. This paper presents the cross section measurements for e$^-$p NC DIS with longitudinally polarised electron beams. The measurements are based on data with an integrated luminosity of 122 pb^{-1} collected at a mean luminosity weighted polarisation of +0.33 and -0.27 with the ZEUS detector in 2004 and 2005. During this time HERA collided protons of energy 920 GeV with electrons of energy 27.5 GeV, yielding collisions at a centre-of-mass energy of 318 GeV.

2 Kinematic variables and cross sections

Inclusive deep inelastic lepton-proton scattering can be described in terms of the kinematic variables x, y and Q^2. The variable Q^2 is defined to be $Q^2 = -q^2 = -(k - k')^2$ where k and k' are the four-momenta of the incoming and scattered lepton, respectively. Bjorken x is defined by $x = Q^2/2P \cdot q$ where P is the four-momentum of the incoming proton. The variables x, y and Q^2 are related by $Q^2 = sxy$, where $s = 4E_eE_p$ is the square of the lepton-proton centre-of-mass energy (neglecting the masses of the incoming particles).

The unpolarised electroweak Born-level cross section for the $e^{\pm}p$ NC interaction can be written as [17]

$$\frac{d^2\sigma(e^{\pm}p)}{dxdQ^2} = \frac{2\pi\alpha^2}{xQ^4}[Y_+F_2(x,Q^2) \mp Y_-xF_3(x,Q^2) - y^2F_L(x,Q^2)] \qquad (1)$$

where α is the fine-structure constant, $Y_{\pm} \equiv 1 \pm (1-y)^2$, and $F_2(x,Q^2)$, $F_3(x,Q^2)$ and $F_L(x,Q^2)$ are the structure functions. The F_2 contribution dominates the cross section at low Q^2, while F_3 starts to contribute only at high Q^2 as it arises from γ/Z^0 interference and pure Z^0 exchange. The F_2 and F_3 structure functions are defined in Eqs. (3) and (4). The F_L contribution can be ignored as it is small in the kinematic region considered.

The reduced cross section is defined as

$$\tilde{\sigma}^{e^\pm p} = \frac{xQ^4}{2\pi\alpha^2}\frac{1}{Y_+}\frac{d^2\sigma(e^\pm p)}{dxdQ^2} = F_2(x,Q^2) \mp \frac{Y_-}{Y_+}xF_3(x,Q^2)$$

which can be used to extract xF_3

$$xF_3(x,Q^2) = \frac{Y_+}{2Y_-}(\tilde{\sigma}^{e^-p} - \tilde{\sigma}^{e^+p}). \tag{2}$$

The NC cross section is modified when the incoming lepton beam is longitudinally polarised. The longitudinal polarisation is defined as

$$P_e = \frac{N_R - N_L}{N_R + N_L}$$

where N_R and N_L are the numbers of right and left-handed leptons in the beam. The Born e^-p NC cross section defined by Eq. (1) can be generalised as

$$\frac{d^2\sigma(e^-p)}{dxdQ^2} = \frac{2\pi\alpha^2}{xQ^4}[H^- + P_e H^-_{P_e}]$$

where F_L is ignored and H^- and $H^-_{P_e}$ contain the unpolarised and polarised structure functions, respectively,

$$H^- = Y_+F_2(x,Q^2) + Y_-xF_3(x,Q^2), \qquad H^-_{P_e} = Y_+F_2^{P_e}(x,Q^2) + Y_-xF_3^{P_e}(x,Q^2).$$

At leading order in QCD the structure functions can be written in terms of parton density functions (PDFs) as

$$F_2(x,Q^2) = \sum_q x(q(x,Q^2) + \bar{q}(x,Q^2))A_q(Q^2) \tag{3}$$

$$xF_3(x,Q^2) = \sum_q x(q(x,Q^2) - \bar{q}(x,Q^2))B_q(Q^2) \tag{4}$$

and

$$F_2^{P_e}(x, Q^2) = \sum_q x(q(x, Q^2) + \bar{q}(x, Q^2))A_q^{P_e}(Q^2)$$

$$xF_3^{P_e}(x, Q^2) = \sum_q x(q(x, Q^2) - \bar{q}(x, Q^2))B_q^{P_e}(Q^2)$$

where the sums run over the quark flavours from $u \ldots b$. The $A^{(P_e)}(Q^2)$ and $B^{(P_e)}(Q^2)$ coefficients contain the quark and electron couplings to the photon and the Z^0 boson and are defined elsewhere [17].

The single differential cross sections in x, y and Q^2 and the reduced cross sections for positively and negatively longitudinally polarised electrons are presented. The reduced cross sections are combined with previous NC measurements to extract xF_3 using Eqn. (2).

3 Monte Carlo simulation

Monte Carlo simulation (MC) was used to determine the efficiency for selecting events, the accuracy of kinematic reconstruction, to estimate the background rate, and to deduce cross sections for the full kinematic region from the data. The MC samples were normalised to the total integrated luminosity of the data.

NC DIS events including radiative effects were simulated using the DJANGOH 1.3 [18] generator. The hadronic final state was simulated using the colour-dipole model of ARIADNE 4.10 [19] and, as a systematic check, the MEPS model of LEPTO 6.5 [20]. Both programs use the Lund string model of JETSET 7.4 [21] for the hadronisation. Photoproduction background was estimated using events simulated with HERWIG 5.9 [22].

4 Event reconstruction and selection

ZEUS is a multipurpose detector described in detail elsewhere [23]. The NC events detected are characterised by the presence of a high-energy isolated scattered electron. The hadronic transverse momentum of the event is calculated by

$$P_{T,h}^2 = P_{x,h}^2 + P_{y,h}^2 = \left(\sum_i^h E_i \sin\theta_i \cos\phi_i\right)^2 + \left(\sum_i^h E_i \sin\theta_i \sin\phi_i\right)^2$$

where the sum runs over all calorimeter energy deposits, E_i, excluding the scattered electron. The polar and azimuthal angles of the energy deposits, θ_i and ϕ_i, are defined from the interaction vertex[1].

The hadronic polar angle, γ_h, is defined by

$$\cos\gamma_h = \frac{P_{T,h}^2 - \delta_h^2}{P_{T,h}^2 + \delta_h^2}$$

where

$$\delta_h = \sum_i^h (E_i - E_i\cos\theta_i) = \sum_i^h (E - P_z)_i. \qquad (5)$$

The variable δ is defined analogously to Eq. (5) but the sum also includes the scattered electron measurements. It follows from longitudinal momentum conservation that for well measured NC DIS events δ peaks at twice the electron beam energy, i.e. 55 GeV.

The double-angle method [24] was used to estimate the kinematic variables from the polar angle of the scattered electron and γ_h.

The following criteria were imposed to select NC events and reject background:

- electron identification: an algorithm which combined information from the energy deposits in the calorimeter with tracks measured in the central tracking detectors was used to identify scattered electrons. A fiducial-volume cut was applied to guarantee that the experimental acceptance was well understood. To ensure high purity and reject background, the identified electron was required to have an energy of at least 10 GeV and be isolated such that the energy not associated with the electron in an $\eta - \phi$ cone of radius 0.8 centred on the electron was less than 5 GeV. A track matched to the energy deposit in the calorimeter was required for events in which an electron was found within the acceptance of the central tracking detector (CTD). The track requirement was replaced with the requirement that the transverse momentum of the electron exceeded 30 GeV for events with an electron at a polar angle smaller than the CTD's acceptance;
- primary vertex: events were required to satisfy $|Z_{\rm vtx}| < 50$ cm. The Z coordinate of the ep interaction vertex, reconstructed using tracks in the central tracking detectors, was required to be in the centre of the detector;
- background rejection: the requirement $38 < \delta < 65$ GeV was imposed to remove photoproduction and beam-gas events, and to reduce the number of events with significant QED initial state radiation. To further reduce background from photoproduction

[1] The ZEUS coordinate system is a right-handed Cartesian system, with the Z axis pointing in the proton beam direction, the Y axis pointing up, and the X axis pointing towards the centre of HERA. The polar angle, θ, is measured with respect to the proton beam direction. The coordinate origin is at the nominal interaction point.

events, y calculated from the electron method, y_e, was required to satisfy $y_e < 0.95$. The net transverse momentum is expected to be small, so in order to remove cosmic-ray events and beam-related background events the quantity $P_T/\sqrt{E_T}$ was required to be less than $4\sqrt{\text{GeV}}$, and the quantity P_T/E_T was required to be less than 0.7;

- QEDC rejection: elastic Compton scattering events were rejected to reduce the size of the QED radiative corrections;
- kinematic region: the final event sample was defined by requiring Q^2 calculated from the double-angle method, Q^2_{DA}, satisfied $Q^2_{\text{DA}} > 200\,\text{GeV}^2$.

A total of 225265 candidate events passed the selection criteria. The background contamination estimated from photoproduction MC was typically less than 1%. Figure 1 presents a comparison of distributions between data and MC, showing that the MC describes the data well.

5 Cross section determination

The measured cross section in a particular kinematic bin, for example in $d\sigma/dQ^2$, was determined from

$$\frac{d\sigma}{dQ^2} = \frac{N_{\text{data}} - N_{\text{bg}}}{N_{\text{MC}}} \cdot \frac{d\sigma^{\text{SM}}_{\text{Born}}}{dQ^2}$$

where N_{data} is the number of data events, N_{bg} is the number of background events estimated from the MC simulation and N_{MC} is the number of signal MC events. The bin sizes used for the determination of the single and double differential cross sections were chosen to be well matched to the resolutions.

The major source of systematic uncertainty in the NC cross section was the uncertainty in the parton-shower scheme which gave changes in the cross section of typically 5% and up to 13% at high Q^2. The systematic effects of the selection cuts were estimated by varying the threshold value of each selection cut independently by typically 10%, corresponding reasonably to the resolution. The resulting shifts in the cross sections were typically within $\pm 5\%$.

The individual uncertainties were added in quadrature separately for the positive and negative deviations from the nominal cross section values to obtain the total systematic uncertainty. The electron beam polarisation was measured using the HERA Compton polarimeters [25, 26]. The relative uncertainty was 5% for the measured polarisation and 3.5% for the measured luminosity, and these uncertainties were not included in the total systematic uncertainty.

6 Results

The single differential cross section $d\sigma/dQ^2$ for e^-p NC DIS is shown in Fig. 2 for electron beams with positive and negative longitudinal polarisation, and the ratio of the cross sections. Only statistical uncertainties were considered when taking the ratio. Evidence of parity violation is seen as there is a clear difference between the measurements with positive and negative polarisation which is well described by the SM predictions evaluated using the ZEUS-JETS PDFs. Measurements of $d\sigma/dx$ and $d\sigma/dy$ in the kinematic region $Q^2 > 200\,\mathrm{GeV}^2$ are presented in Figs. 3 and 4, showing an overall shift in the cross section ratio due to the polarisation which is also well described by the SM.

Figure 5 shows the reduced cross sections for e^-p with positive and negative polarisations which are well described by the SM predictions. Reduced cross sections for unpolarised $e^{\pm}p$ are presented in Fig. 6. The e^-p measurement refers to the total data set previously described, with the residual longitudinal polarisation of -0.06 corrected to zero by theoretical predictions. This correction was at most 2% in the highest Q^2 bins. These results are compared with previously measured unpolarised e^+p NC DIS reduced cross sections taken in 1999 and 2000 [12]. A significant difference between the e^-p and e^+p unpolarised cross sections is seen at high Q^2 due to the contribution of xF_3 and is described well by the SM predictions.

Figure 7 shows the structure function xF_3 extracted using the unpolarised e^-p and e^+p reduced cross sections as described in Eq. (2). The measurements are reproduced well by the SM curve based on the ZEUS-JETS PDFs.

7 Summary

The cross sections for NC DIS in e^-p collisions with longitudinally polarised electron beams have been measured for the first time at ZEUS in the kinematic region $Q^2 > 200\,\mathrm{GeV}^2$. The measurements are based on e^-p data with an integrated luminosity of $122\,\mathrm{pb}^{-1}$ collected with the ZEUS detector in 2004 and 2005 at a centre-of-mass energy of $318\,\mathrm{GeV}$. The e^-p cross sections have been combined with previously measured unpolarised e^+p NC DIS cross sections to extract xF_3.

The SM predictions describe the measurements well and this is the first time at ZEUS that parity violation can clearly be seen in the $d\sigma/dQ^2$ measurement.

References

[1] H1 Coll., S. Aid et al., Phys. Lett. **B 379**, 319 (1996).

[2] H1 Coll., S. Aid et al., Nucl. Phys. **B 470**, 3 (1996).

[3] H1 Coll., C. Adloff et al., Nucl. Phys. **B 497**, 3 (1997).

[4] H1 Coll., C. Adloff et al., Eur. Phys. J. **C 13**, 609 (2000).

[5] H1 Coll., C. Adloff et al., Eur. Phys. J. **C 19**, 269 (2001).

[6] H1 Coll., C. Adloff et al., Eur. Phys. J. **C 21**, 33 (2001).

[7] H1 Coll., C. Adloff et al., Eur. Phys. J. **C 30**, 1 (2003).

[8] ZEUS Coll., M. Derrick et al., Phys. Rev. Lett. **75**, 1006 (1995).

[9] ZEUS Coll., J. Breitweg et al., Eur. Phys. J. **C 11**, 427 (1999).

[10] ZEUS Coll., S. Chekanov et al., Eur. Phys. J. **C 21**, 443 (2001).

[11] ZEUS Coll., S. Chekanov et al., Eur. Phys. J. **C 28**, 175 (2003).

[12] ZEUS Coll.; S. Chekanov et al., Phys. Rev. **D 70**, 052001 (2004).

[13] NMC Coll., M. Arneodo et al., Nucl. Phys. **B 483**, 3 (1997).

[14] BCDMS Coll., A.C. Benvenuti et al., Phys. Lett. **B 223**, 485 (1989).

[15] E665 Coll., M.R. Adams et al., Phys. Rev. **D 54**, 3006 (1996).

[16] ZEUS Coll., S. Chekanov et al., Preprint hep-ex/0402026, 2006. Accepted by Phys. Lett. B.

[17] R. Devenish and A. Cooper-Sarkar, *Deep Inelastic Scattering*. Oxford University Press, 2003.

[18] G.A. Schuler and H. Spiesberger, *Proc. Workshop on Physics at HERA*, W. Buchmüller and G. Ingelman (eds.), Vol. 3, p. 1419. Hamburg, Germany, DESY (1991);
H. Spiesberger, HERACLES *and* DJANGOH*: Event Generation for ep Interactions at HERA Including Radiative Processes*, 1998, available on `http://www.desy.de/~hspiesb/djangoh.html`.

[19] L. Lönnblad, Comp. Phys. Comm. **71**, 15 (1992).

[20] G. Ingelman, A. Edin and J. Rathsman, Comp. Phys. Comm. **101**, 108 (1997).

[21] T. Sjöstrand, Comp. Phys. Comm. **39**, 347 (1986);
T. Sjöstrand and M. Bengtsson, Comp. Phys. Comm. **43**, 367 (1987);
T. Sjöstrand, Comp. Phys. Comm. **82**, 74 (1994).

[22] G. Marchesini et al., Comp. Phys. Comm. **67**, 465 (1992).

[23] ZEUS Coll., U. Holm (ed.), *The ZEUS Detector*. Status Report (unpublished), DESY (1993), available on `http://www-zeus.desy.de/bluebook/bluebook.html`.

[24] S. Bentvelsen, J. Engelen and P. Kooijman, *Proc. Workshop on Physics at HERA*, W. Buchmüller and G. Ingelman (eds.), Vol. 1, p. 23. Hamburg, Germany, DESY (1992);
K.C. Höger, *Proc. Workshop on Physics at HERA*, W. Buchmüller and G. Ingelman (eds.), Vol. 1, p. 43. Hamburg, Germany, DESY (1992).

[25] M. Beckmann et al., Nucl. Inst. Meth. **A 479**, 334 (2002).

[26] D.P. Barber et al., Nucl. Inst. Meth. **A 329**, 79 (1993).

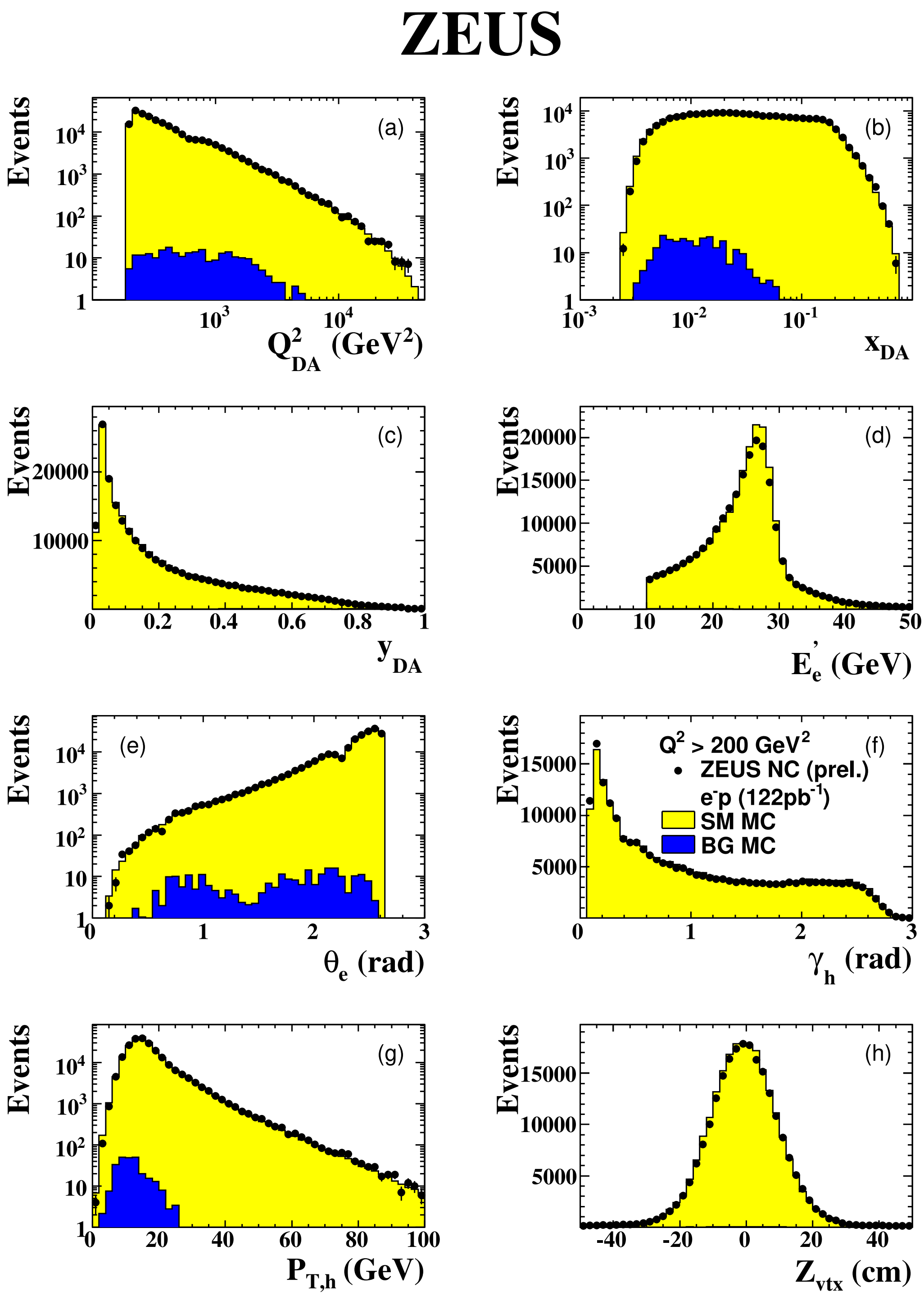

Figure 1: *Comparison of the final e^-p NC data sample with the expectations of the MC simulation described in the text, where BG MC refers to the photoproduction background MC. The distributions of (a) $Q^2_{\rm DA}$, (b) $x_{\rm DA}$, (c) $y_{\rm DA}$, (d) the energy of the scattered electron, E'_e, (e) the angle of the scattered electron, θ_e, (f) the hadronic angle , γ_h, (g) the transverse momentum of the hadronic system, $P_{T,h}$, and (h) the Z coordinate of the event vertex, Z_{vtx}, are shown.*

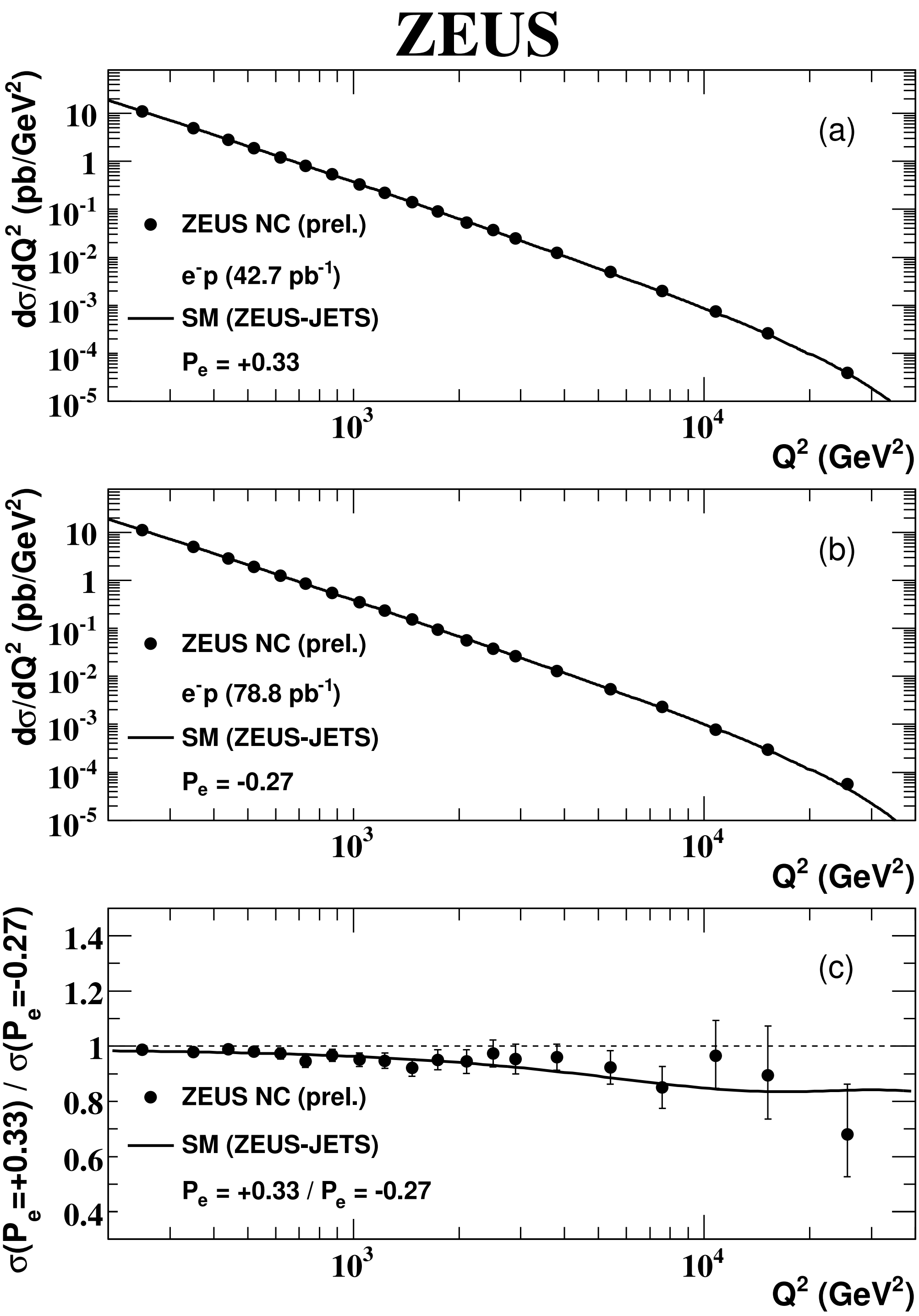

Figure 2: *The e^-p NC DIS cross section $d\sigma/dQ^2$ for (a) positive polarisation data and (b) negative polarisation data and (c) the ratio of the two. The closed circles represent data points and the curves show the predictions of the SM evaluated using the ZEUS-JETS PDFs. Only statistical uncertainties are shown in the cross section ratio.*

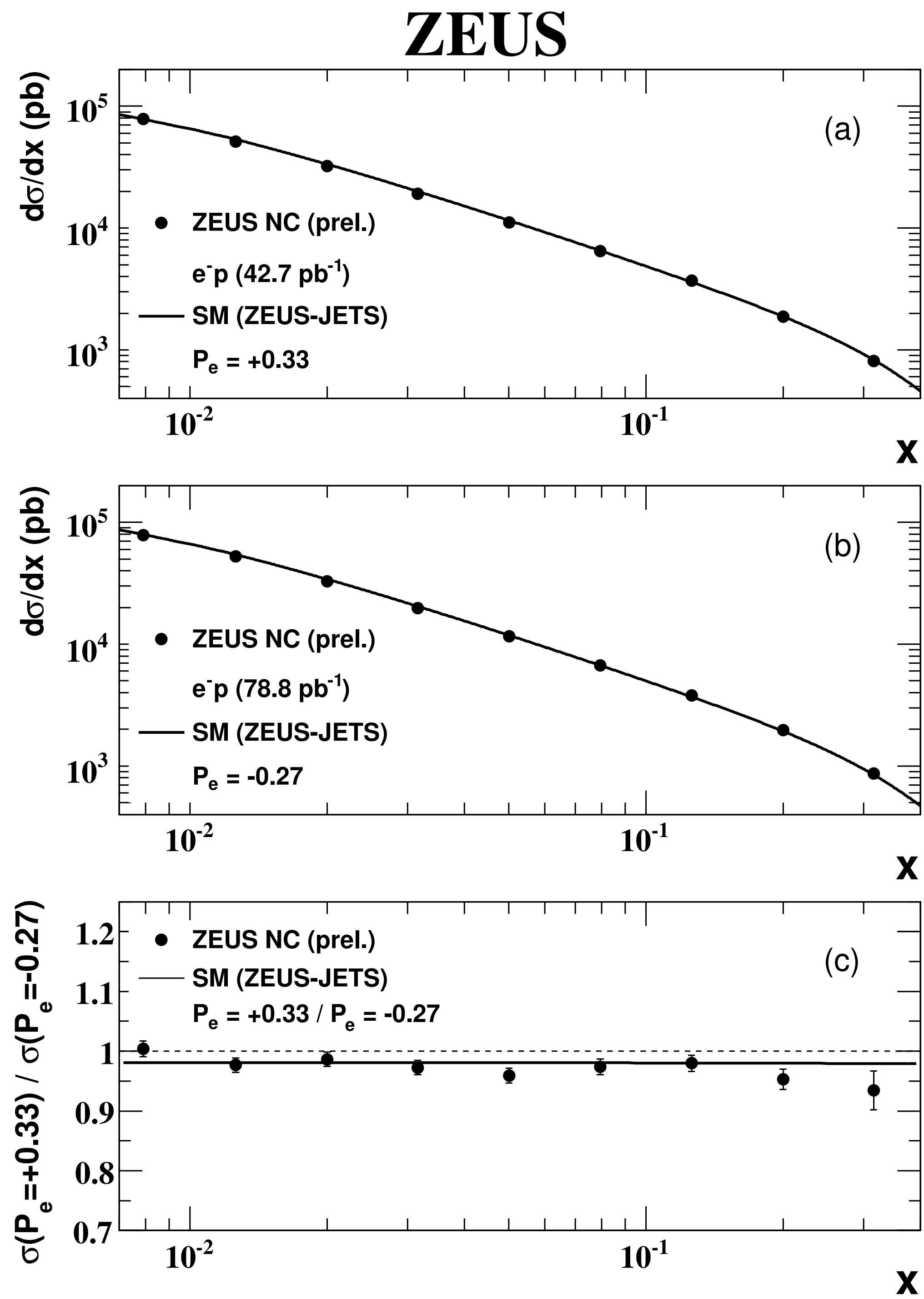

Figure 3: *The $e^{-}p$ NC DIS cross section $d\sigma/dx$ for (a) positive polarisation data and (b) negative polarisation data and (c) the ratio of the two. The closed circles represent data points and the curves show the predictions of the SM evaluated using the ZEUS-JETS PDFs. Only statistical uncertainties are shown in the cross section ratio.*

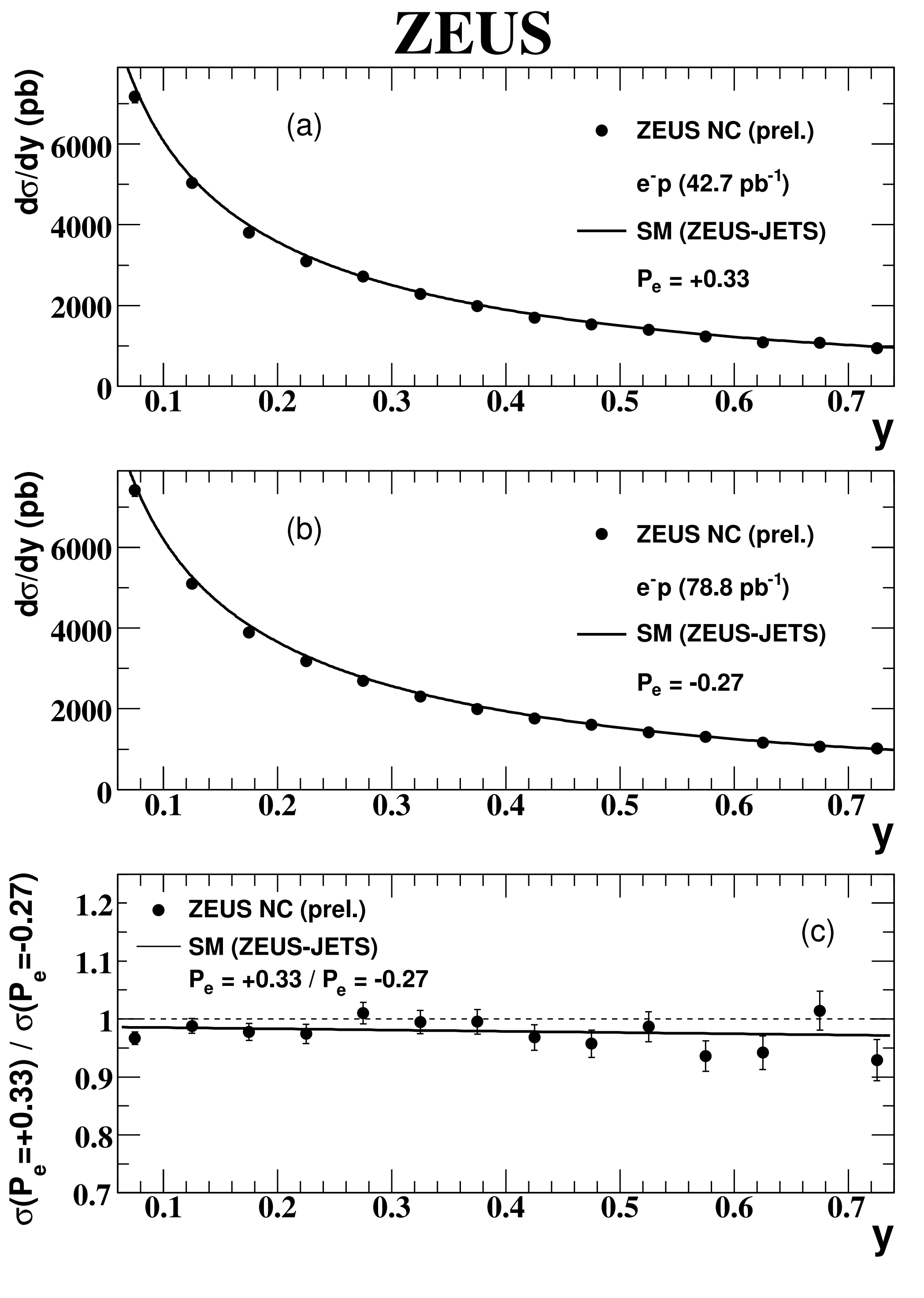

Figure 4: *The e^-p NC DIS cross section $d\sigma/dy$ for (a) positive polarisation data and (b) negative polarisation data and (c) the ratio of the two. The closed circles represent data points and the curves show the predictions of the SM evaluated using the ZEUS-JETS PDFs. Only statistical uncertainties are shown in the cross section ratio.*

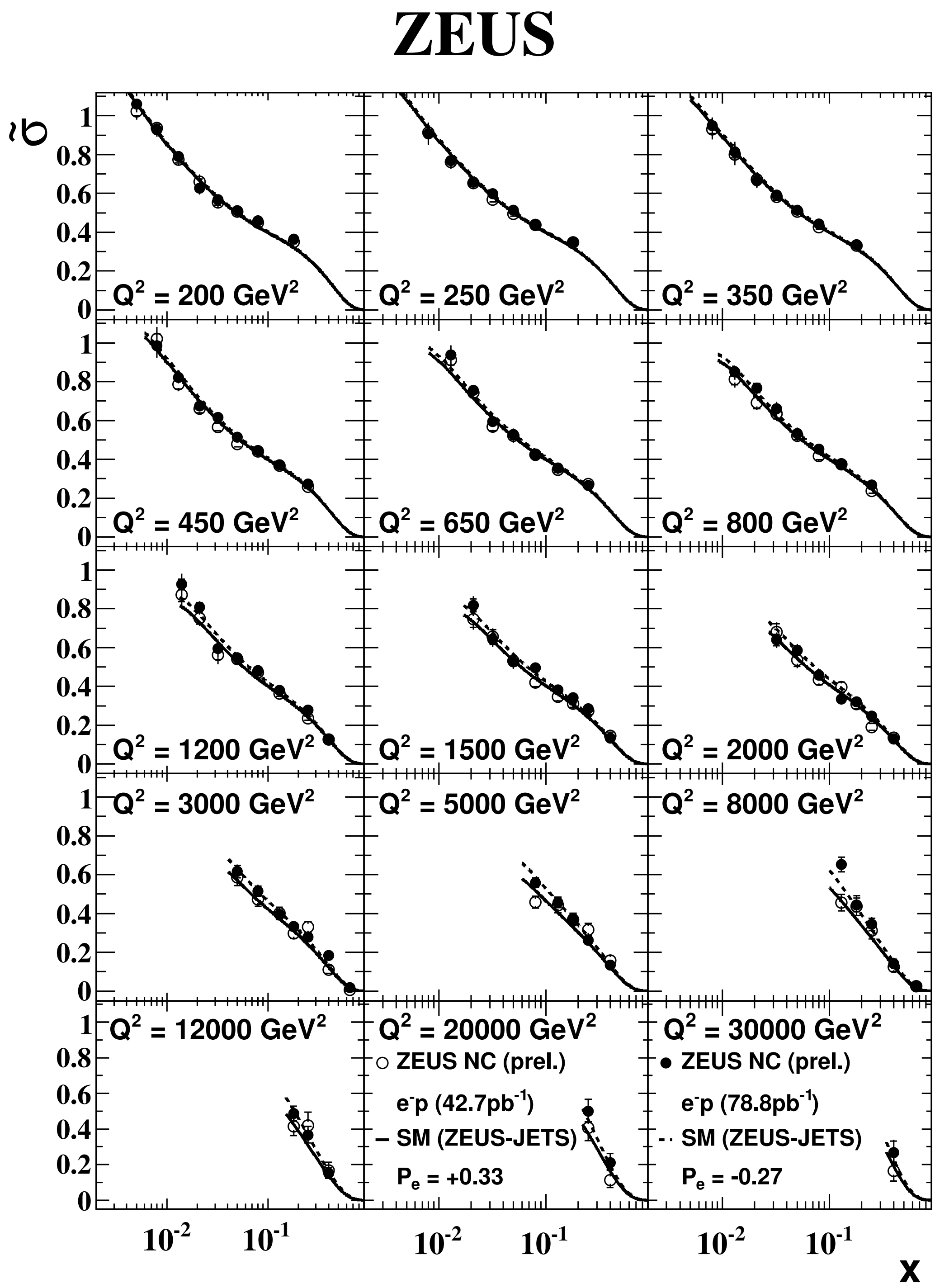

Figure 5: *The e^-p NC DIS reduced cross section, $\tilde{\sigma}$, for positively and negatively polarised data plotted as a function of x in fixed Q^2 bins. The closed (open) circles represent data points for the negative (positive) polarisation measurements and the curves show the predictions of the SM evaluated using the ZEUS-JETS PDFs.*

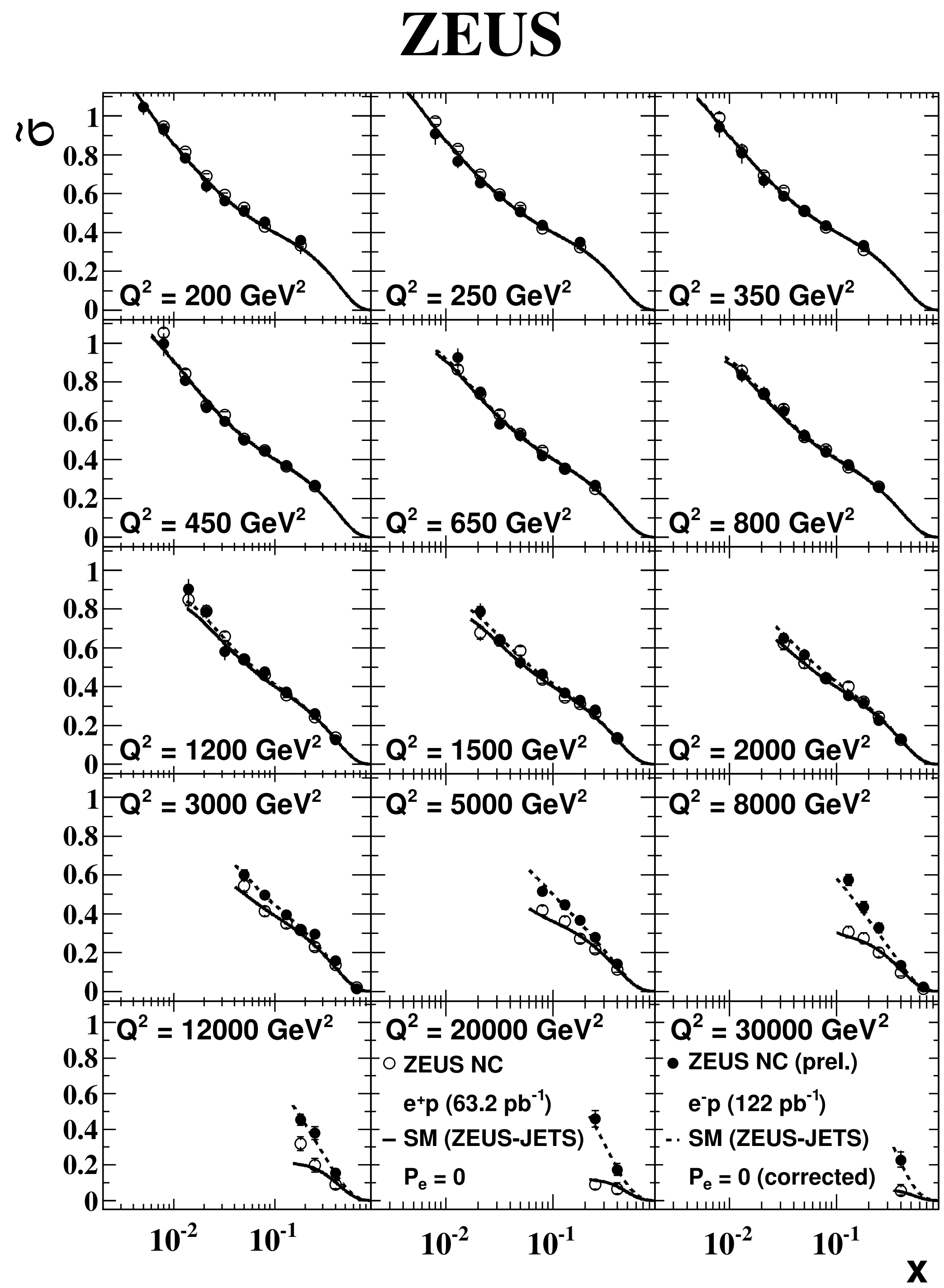

Figure 6: *The $e^{\pm}p$ unpolarised NC DIS reduced cross section, $\tilde{\sigma}$, plotted as a function of x in fixed Q^2 bins. The closed (open) circles represent data points for e^-p (e^+p) collisions and the curves show the predictions of the SM evaluated using the ZEUS-JETS PDFs.*

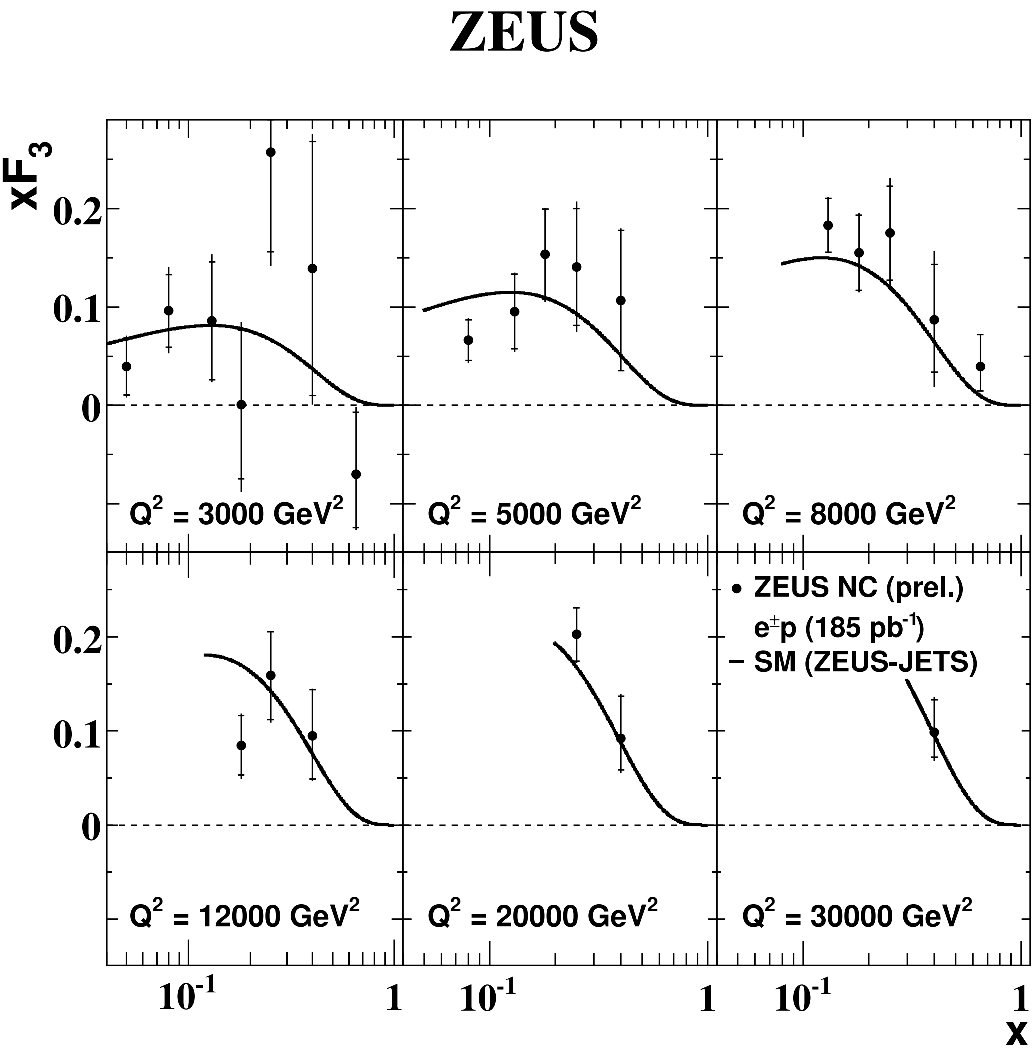

Figure 7: *The structure function xF_3 plotted as a function of x in fixed Q^2 bins. The closed circles represent data points and the curves show the predictions of the SM evaluated using the ZEUS-JETS PDFs. The inner error bars on the data points show the statistical uncertainty, while the outer ones show the statistical and systematic uncertainties added in quadrature.*